Characterizing Edible Oils by Oblique-Incidence Reflectivity Difference Combined with Machine Learning Algorithms

Xiaorong Sun , Yiran Hu , Cuiling Liu * , Shanzhe Zhang , Sining Yan , Xuecong Liu , Kun Zhao *

Posted Date: 3 April 2024

doi: 10.20944/preprints202404.0285.v1

Keywords: Oblique-incidence reflectivity difference; Edible oils; Machine learning; Feature importance scores

Article

Characterizing Edible Oils by Oblique-Incidence Reflectivity Difference Combined with Machine Learning Algorithms

Xiaorong Sun [1,2], Yiran Hu [1,2], Cuiling Liu [1,2,*], Shanzhe Zhang [1,2], Sining Yan [1,2], Xuecong Liu [3] and Kun Zhao [4,5,*]

[1] College of Computer and Artificial Intelligence, Beijing Technology and Business University. 100048, Beijing
[2] Beijing Key Laboratory of Big Data Technology for Food Safety, Beijing Technology and Business University. 100048, Beijing
[3] College of Information Science and Engineering/College of Artificial Intelligence, China University of Petroleum, Beijing 102249, China
[4] College of New Energy and Materials, China University of Petroleum, Beijing 102249, China
[5] Key Laboratory of Oil and Gas Terahertz Spectroscopy and Photoelectric Detection, Petroleum and Chemical Industry Federation, China University of Petroleum, Beijing 102249, China
* Correspondence: author. E-mail address: zhk@cup.edu.cn; liucl@btbu.edu.cn; Tel:+86 13911712105

Abstract: Due to the significant price difference, expensive oils like olive oil are often blended with cheaper edible oils. This practice of adulteration in edible oils, aimed at increasing profits for producers, poses a major concern for consumers. Furthermore, adulteration in edible oils can lead to various health issues impacting consumer well-being. In order to meet the requirements of fast, non-destructive, universal, accurate and reliable quality testing for edible oil, the oblique-incidence reflectivity difference (OIRD) method combined with machine learning algorithms was introduced to detect a variety of edible oils. The prediction accuracy of Gradient Boosting, K-Nearest Neighbor, and Random Forest models exceeded 95%. Experimental results indicate that the OIRD method can serve as a powerful tool for detecting edible oils.

Keywords: oblique-incidence reflectivity difference; edible oils; machine learning; feature importance scores

1. Introduction

The edible oil plays an important role in our daily life, such as providing essential fatty acids, vitamins, and health promoting ingredients. The annual consumption of edible oil is huge, which reflected the importance of edible oil safety. Due to the influence of raw materials, there is a significant price difference among different types of edible oils. Besides, differences in brand, source of raw materials, and processing techniques resulted in the variations of ingredients and prices. Unscrupulous profit motives have led some businesses to deceive consumers by selling substandard products. Therefore, the safety testing of edible oil is of great importance in food safety assessment.

There are several procedures to research the edible oil in food safety field, such as flash gas chromatography[1–3], TaqMan real-time quantitative polymerase chain reaction[4], gas chromatography ion mobility spectrometry[5,6] and electrochemical impedance spectroscopy[7]. Combined with chemometrics, flash gas chromatography had been used to assess volatile profiles of berry seed oils in terms of the authenticity and the deterioration assessment. The partial least squares model was used to predict storage time, and the results demonstrated that the coefficient of determination (R^2) was between 0.842 and 0.969.1 .Moreover, gas chromatography ion mobility spectrometry was employed to analyze the secondary oxidative, in order to monitor edible oil rancidity and oxidative stability. The predictive model for the peroxide value of rapeseed oil was

 doi:10.20944/preprints202404.0285.v1

established to research the relationships between peroxide values and the contents of secondary oxidative products. Besides, non-destructive ultrasonic method was used to investigate the temperature-dependent of acoustic parameters of edible oils. As oil temperature ranged from 24 ℃ to 34 ℃, acoustic parameters were closely related to the velocity, attenuation, and frequency components present in 2.25 MHz ultrasonic waves.[8]

Recently, with advantages of rapid, collimated and non-contact, optic methods have been widely used in edible oil detection. Fourier Transform Infrared spectroscopy was used to monitor the thermal stability of pure sesame oil and a linear correlation was obtained between the FTIR signals at different conditions and the proportion of pure sesame oil with the root mean square of prediction (RMSEP) between 0.8802 and 2.3827 and R^2 between 0.9841 and 0.8834, respectively.[9] Besides, surface-enhanced Raman spectroscopy, combined with Artificial Neural Network, was used for determination of peroxide value and fatty acid composition with a accuracy of 99%.[10] In addition, fluorescence spectroscopy[11–14], reflectance spectroscopy[15–17] and terahertz spectroscopy[18–21] have been also used in edible oil measurement.

In this work, the oblique-incidence reflectivity difference (OIRD) method was proposed for edible oil detection. The prediction model was performed based on four different algorithms, which included Extreme Gradient Boosting, Logistic Regression, K-Nearest Neighbor and Random Forest. The predicted results showed a clear correspondence with the content of monounsaturated fatty acids. Moreover, the contribution of OIRD signals was significantly higher than that of direct current signals and fundamental frequency signals. Experimental results suggested that OIRD offers a useful tool to detect edible oil.

2. Materials and Methods

In this work five types of edible oils, with six brands for each type, were used for testing. The information of edible oil samples was shown in Table 1.

Table 1. Edible Oil Sample Information.

Types of Edible Oils	Oil 1	Oil 2	Oil 3	Oil 4	Oil 5
corn oil	corn oil 1	corn oil 2	corn oil 3	corn oil 4	corn oil 5
olive oil	olive oil 1	olive oil 2	olive oil 3	olive oil 4	olive oil 5
peanut oil	peanut oil 1	peanut oil 2	peanut oil 3	peanut oil 4	peanut oil 5
rapeseed oil	rapeseed oil 1	rapeseed oil 2	rapeseed oil 3	rapeseed oil 4	rapeseed oil 5
Soybean oil	Soybean oil 1	soybean oil 2	soybean oil 3	soybean oil 4	soybean oil 5

The schematic diagram of the experimental setup for the OIRD was shown in Figure 1. The He-Ne laser was adopted with a power of 3.8 mW and polarization ratio of 500:1. The laser operated at an incident angle corresponded to the Brewster angle (58°) with a 632.8 nm beam. Moreover, the incident light intensity was adjusted using an attenuator. The polarization degree was enhanced using a polarizer to modulate the laser into p-polarized light. The polarization state of the laser was further adjusted by a photo-clastic modulator to introduce s-polarized light at a frequency of 50 kHz. Thus, the s-polarized light and p-polarized light alternately exited the system. Quarter-wavelength Phase shifter introduced a fixed phase difference between the two polarized components of the incident light. The reflected light was focused on the sample using a plano-convex lens. The reflected beam passed through an optical beam splitter, transformed into parallel light by another plano-convex lens, and then reached a silicon photodetector through a polarizer to suppress unwanted polarization. The signal was transmitted via a BNC cable to a lock-in amplifier for further processing. According to the Fresnel principle, when laser light is incident on the sample surface at a fixed angle (Brewster angle), the composition, structure, and density of the sample surface will affect the interface dielectric constant, thereby influencing the laser reflectance.

Preprints.org (www.preprints.org) | NOT PEER-REVIEWED | Posted: 3 April 2024 doi:10.20944/preprints202404.0285.v1

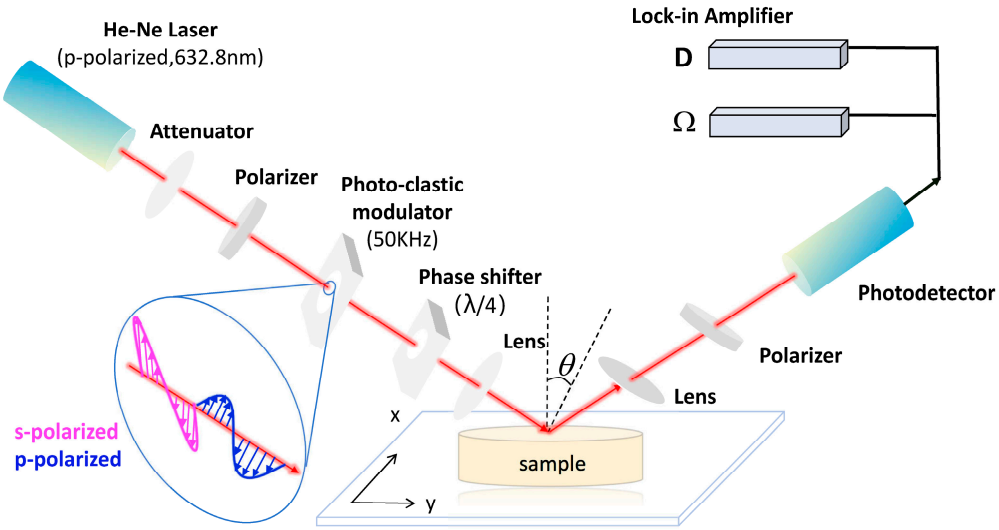

Figure 1. Schematic Diagram of OIRD.

According to the Fresnel principle, when laser light is incident on the sample surface at a fixed angle (Brewster angle), the composition, structure, and density of the sample surface will affect the interface dielectric constant, thereby influencing the laser reflectance. The OIRD technique introduces two alternately emitted, mutually perpendicular linearly polarized lights (p and s) to the sample surface. It detects changes in the properties of the sample interface layer, such as thickness and dielectric constant. The Oblique-incidence reflectivity difference is defined as:

$$\Delta \mathrm{p} - \Delta s = \frac{r_p - r_{p0}}{r_{p0}} - \frac{r_s - r_{s0}}{r_{s0}} = \frac{\delta r_p}{r_{p0}} - \frac{\delta r_s}{r_{s0}} \tag{1}$$

Using the transfer matrix method allows for a quantitative analysis of the interaction process between light and matter, subsequently enabling the calculation of the reflection coefficients r_p and r_s for p-polarized and s-polarized light on the sample. By incorporating equation (1), a quantitative expression for the Optical Interference Reflectance Difference (OIRD) signal in relation to the physical properties of the sample can be derived.

$$\Delta \mathrm{p} - \Delta s = d \frac{(\varepsilon_d - \varepsilon_0)(\varepsilon_d - \varepsilon_s)}{\varepsilon_d} \frac{(-i)4\pi\sqrt{\varepsilon_0}\varepsilon_s \cos\varphi_{inc} \sin^2\varphi_{inc}}{\lambda(\varepsilon_s - \varepsilon_0)\left(\varepsilon_s \cos^2\varphi_{inc} - \varepsilon_0 \sin^2\varphi_{inc}\right)} \tag{2}$$

In this context, where λ represents the wavelength of the incident laser, φ_{inc} denotes the incidence angle of the probing laser, and d signifies the thickness of the interface layer, while ε_0、ε_d and ε_s respectively represent the dielectric constants of the overlying layer, interface layer, and substrate. According to the Optical Interference Reflectance Difference (OIRD) monitoring mechanism, based on the direct current signal and the fundamental frequency signal (modulation frequency at 50 kHz) output by the lock-in amplifier, the difference in relative changes in laser reflectance can be obtained:

$$\mathrm{Im}(\Delta p - \Delta s) \approx \frac{1}{2J_1(\pi)}\left(\frac{I(\Omega)}{I_{DC}}\right) \tag{3}$$

When the modulation frequency is fixed, the x-th order Bessel function $J_x(A)$ becomes a constant. Combined with equation (3), when the incident light wavelength λ and the incidence angle φ_{inc}

 doi:10.20944/preprints202404.0285.v1

are constant, and the dielectric properties of the overlying layer and substrate are known, the Optical Interference Reflectance Difference (OIRD) technique can quantitatively detect the interface thickness and dielectric properties.

To ensure the edible oil samples remained relatively stable over time, the single-point dynamic monitoring mode of the OIRD testing system was employed, and the estimated duration of each experimental test was set between 120 and 150 seconds. The output data was formatted as a 2n×2 text document. The direct current signal I_{DC} and the fundamental frequency signal I(Ω=50 kHz) were acquired through the lock-in amplifier. Subsequently, the OIRD signal was derived, and these three signals were employed as features for modeling analysis.

The physical properties were investigated by introducing laser into liquid samples and exploring the differences in reflectance values at the interface. However, scattering inevitably occurred in this process. Multi-scattering correction (MSC), as a data processing method, was designed to eliminate the influence of different scattering levels in the sample, which effectively enhanced data correlation and corrected the baseline shift and offset phenomena in the data by using ideal OIRD data. In this experiment, it was assumed that the average value of the OIRD data serves as the ideal OIRD data.

The resistance of multiple scattering correction to signal noise was limited. Thus, it cannot completely eliminate the scattering noise in the data. Moreover, OIRD signal was susceptible to external noise signals. Savitzky-Golay (S-G) smoothing algorithm was suitable for data preprocessing. S-G smoothing algorithm performed low-pass filtering on information to remove high-frequency components, which can effectively retain low-frequency information.[22] Therefore, the noise was significantly suppressed.

In this work, four machine learning algorithms, including eXtreme Gradient Boosting (XGBoost), Random Forest (RF), Logistic regression (LR) and K-Nearest Neighbors (KNN), were employed in the data processing section to assist us in classification and feature importance scoring.XGBoost was an algorithm based on the Gradient Boosting Decision Tree (GBDT). In each iteration, GBDT learned a CART tree, fitting the difference between the predicted values of the preceding (t-1) trees and the true values of the training set.[23–25] The Random Forest algorithm combines Breiman's "Boot-strap aggregating" idea with Ho's "random subspace" method. RF was a classifier composed of multiple decision trees, and its output category was determined by the majority class among the individual tree outputs.[26,27] Logistic regression was a linear model derived from the exponential distribution family. It assumes that given the input X, the output Y follows a Bernoulli distribution. By introducing the Sigmoid function as a non-linear factor, logistic Regression was widely used in classification problems.[28,29] The K-Nearest Neighbors classifier was an online classifier that, during classification, identifies the K samples in the training set that are closest to the test sample and determines the class of the test sample based on these neighbors.[30]

3. Results and Discussions

The OIRD time-domain signal was described in Figure 2. The signal of single sample exhibited stability, while there were significant differences in OIRD signals among different edible oil samples. For corn oil 1, the OIRD signal Im(Δp-Δs) ranged from 0.2878 to 0.288. The Im(Δp-Δs) of corn oil 2 changed from 0.2851 to 0.2853. Moreover, the Im(Δp-Δs) of oilve oil 1, peanut oil 1, rapeseed oil 1, soybean oil 1 fluctuated around 0.2882, 0.2869, 0.2843 and 0.2864, respectively.

 doi:10.20944/preprints202404.0285.v1

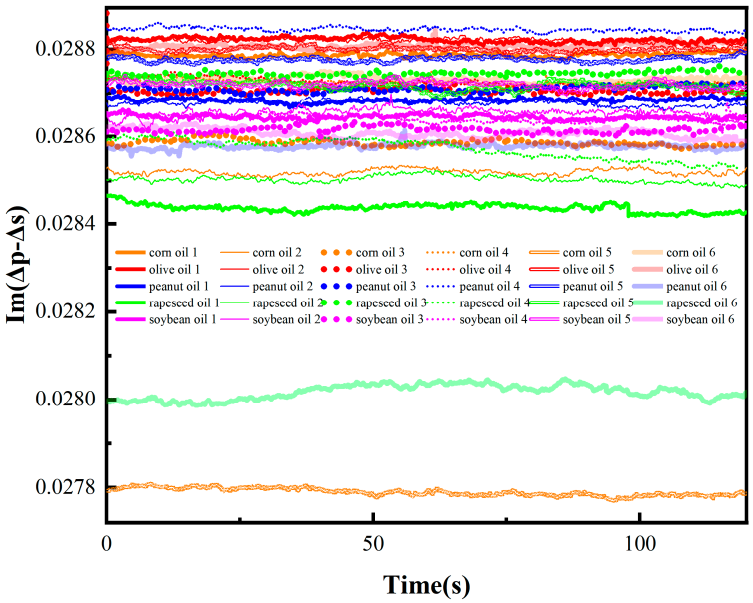

Figure 2. The temporal signals of OIRD for 30 edible oil samples.

The average imaginary signals Im(Δp−Δs) were described in Figure 3. Except for the significantly lower OIRD signals of olive oil samples, it was hardly to distinguish different edible oil samples. This may be attributed to the considerably higher content of monounsaturated fatty acids in olive oil compared to others, leading to a lower dielectric constant in the interface layer of olive oil[31], consequently exhibiting a lower OIRD response. The fatty acid contents of different edible oils were shown in Table 2.

Table 2. the fatty acid content in edible oils.

Reference table for the fatty acid content in edible oils (%)				
edible oils	**Saturated fatty acids**	**Monounsaturated fatty acids**	**Polyunsaturated fatty acids**	
		Oleic acid (Ω-9)	**Linoleic acid (Ω-6)**	**Alpha-linolenic acid (Ω-3)**
corn oil	10-13	20-25	50-60	4-6
olive oil	9-11	67-75	10-15	0-3
peanut oil	17-18	30-40	30-40	0-3
rapseed oil	5-10	40-60	10-20	5-8
Soybean oil	10-13	20-25	55-60	4-6

Preprints.org (www.preprints.org) | NOT PEER-REVIEWED | Posted: 3 April 2024 doi:10.20944/preprints202404.0285.v1

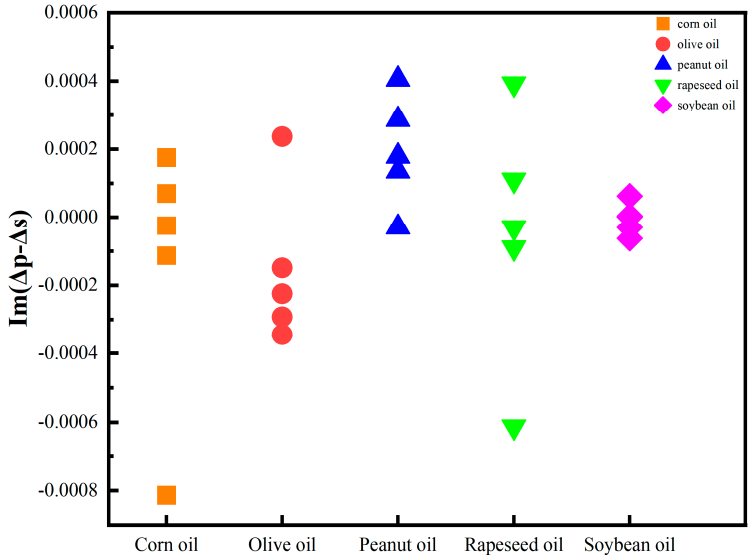

Figure 3. The average OIRD signal of edible oil samples.

The average OIRD signal was taken as the ideal OIRD signal, and a multivariate scatter correction was applied to all OIRD data. This correction involved baseline shift and offset correction of the data based on the ideal OIRD data. Subsequently, the data after multivariate scatter correction were subjected to the S-G smoothing process. After iteratively comparing different parameter combinations for the smoothing model, the polynomial order and the number of smoothing points were set as 7 and 299 in order to achieve the best smoothing effect. The preprocessing effectively eliminated the influence of different scattering levels in the samples and removed external high-frequency noise. Figure 4a–e displayed the OIRD signals of corn oil, olive oil, peanut oil, rapeseed oil and soybean oil after preprocessing, respectively.

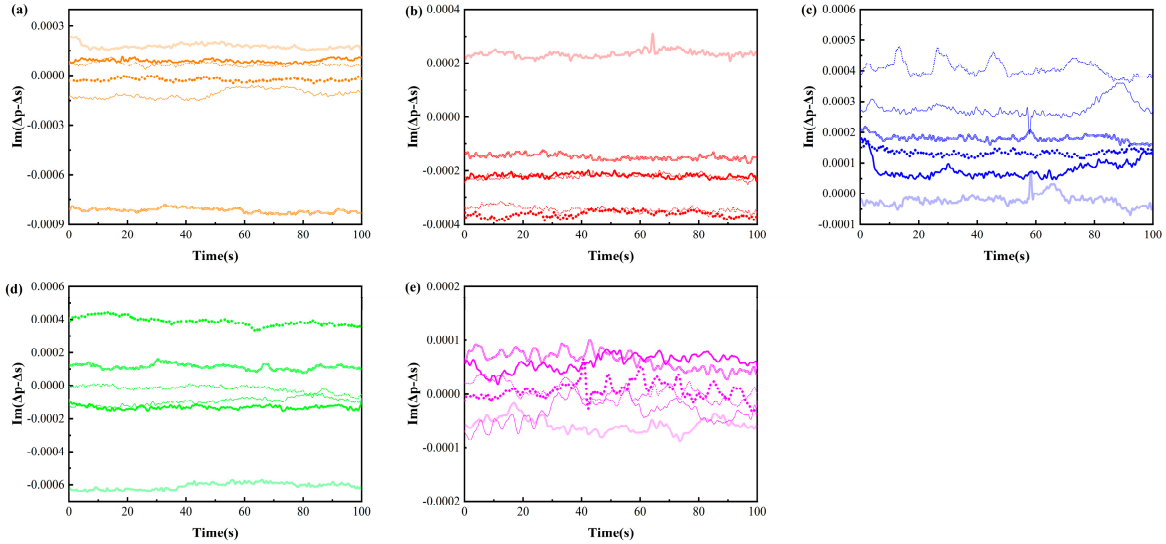

Figure 4. The OIRD temporal signals of five edible oils after preprocessing with S-G+MSC.

DC signal, fundamental frequency signal, and OIRD signal were selected as features in the experiment. The experiment adopted single-point dynamic scanning, and the continuous signal collection for each sample lasted for 120-150 seconds. To ensure the reliability of the results, six oil samples from different origins and brands were collected for each type of edible oil. Finally, approximately 50,000 stable sample points were selected for each type of edible oil as the dataset, in

 doi:10.20944/preprints202404.0285.v1

which 35,000 sample points was used for training and the others for prediction. Confusion matrices and prediction results were described in the Figures 5 and 6. It can be observed that except for LR, the accuracy of the other models in predicting the types of edible oils exceeds 95%. The lower accuracy of the LR model may be attributed to the complex relationships and interactions present in the interface layer dielectric constant and interface layer thickness, which are not simply linear. Additionally, the LR model exhibited limitations in handling continuous and discrete features, which resulted in suboptimal classification performance.

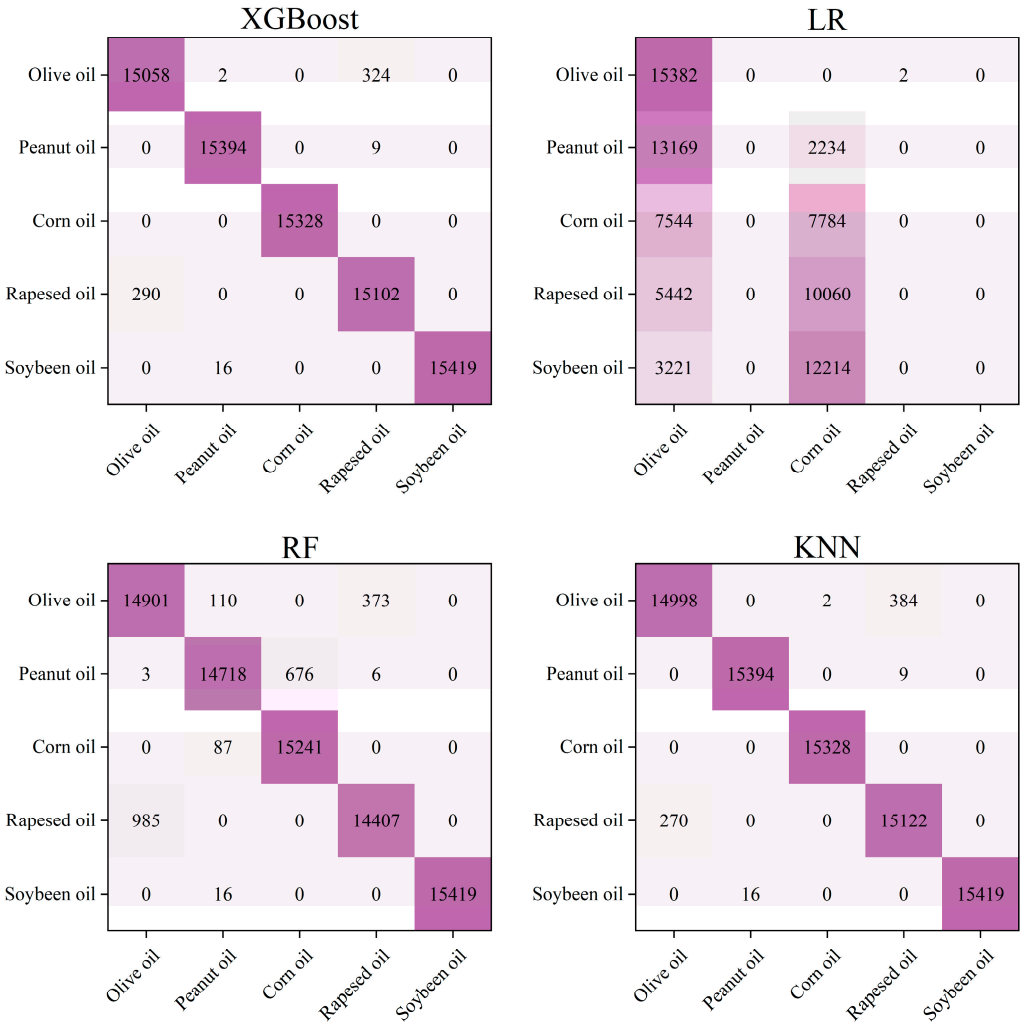

Figure 5. Confusion matrices for predicting the types of edible oils using four models.

Preprints.org (www.preprints.org) | NOT PEER-REVIEWED | Posted: 3 April 2024 doi:10.20944/preprints202404.0285.v1

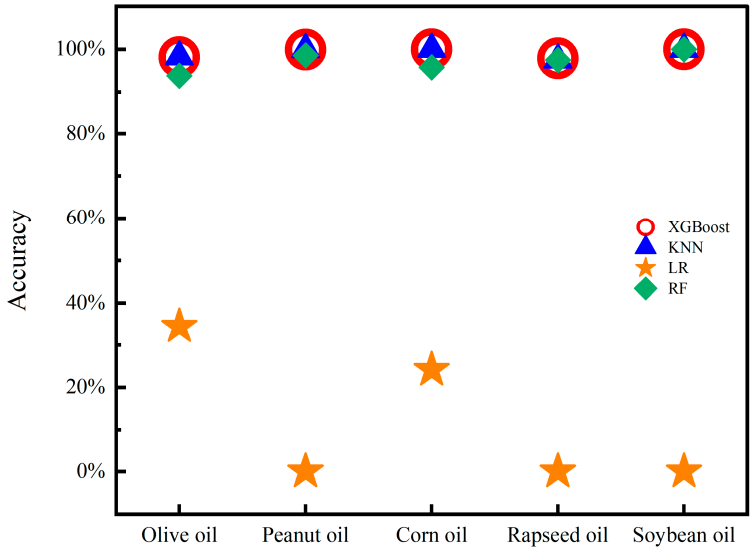

Figure 6. Accuracy of edible oil type prediction.

The predictive performance of XGBoost among the four models is exceptionally good, with an accuracy exceeding 97% for all types of edible oils. As a gradient boosting algorithm, XGBoost improved model performance by ensemble learning from multiple decision trees. And then, non-linear relationships can be analyzed by XGBoost algorithm in order to achieve excellent predictive results. Due to external noise and potential data loss in the test, XGBoost algorithm was used to handle missing values, which can enhance the reliability of prediction outcomes. Feature importance analysis had been conducted using XGBoost algorithm and the feature importance scores for the three signals were shown in the Figure 7. The contribution rates of OIRD signal, DC signal, and fundamental frequency signal to the classification results were 45.7%, 34.1%, and 20.2%, respectively. Both DC signal and fundamental frequency signal were optical intensity signals received by the photodetector and amplified by the lock-in amplifier, which contributed less to the model's predictive accuracy. In contrast, the OIRD signal was calculated from the DC and fundamental frequency signals according to the principles of OIRD technology, which can be expressed by the following relationship equation:

$$\frac{1}{2J_1(\pi)}\left(\frac{I(\Omega)}{I_{DC}}\right)=\frac{(-i)4\pi d\sqrt{\varepsilon_0}\varepsilon_s\cos\varphi_{inc}\sin^2\varphi_{inc}}{\lambda(\varepsilon_s-\varepsilon_0)\left(\varepsilon_s\cos^2\varphi_{inc}-\varepsilon_0\sin^2\varphi_{inc}\right)}\frac{(\varepsilon_d-\varepsilon_0)(\varepsilon_d-\varepsilon_s)}{\varepsilon_d} \tag{4}$$

The results indicated that the alone use of either DC or fundamental frequency signals did not effectively characterize the samples. However, the OIRD signal can be derived from the ratio of the two signals. Under the conditions of a fixed incident angle and modulation frequency of the photoelastic modulator, the OIRD signal can reflect both the thickness and dielectric properties of the interface layer. Moreover, it can characterize the complex interplay between these two aspects. Applying the interface properties to differentiate types of edible oils exhibited high accuracy, which can provide a novel method for addressing this issue.

 doi:10.20944/preprints202404.0285.v1

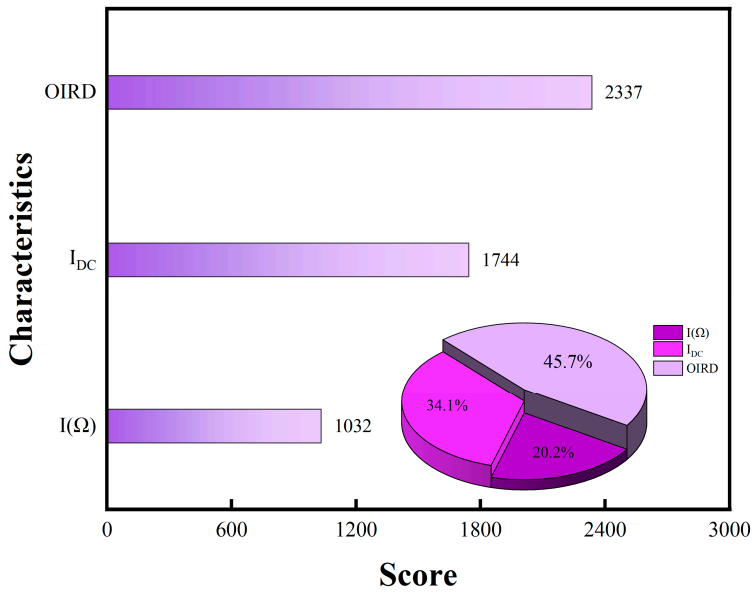

Figure 7. XGBoost feature importance scores for predicting the types of edible oils.

Using single-point dynamic scanning, DC, fundamental frequency and OIRD signals were collected from six olive oil samples, which originated from different brands and regions. XGBoost, LR, RF and KNN models were employed for quality analysis of the six olive oil samples. Each sample underwent continuous signal acquisition for 120–150 seconds. For each type of olive oil, approximately 10,000 stable sample points were selected as the dataset, while 7,000 sample points were used for training and the others were used for prediction. Confusion matrices and prediction results were shown in the Figures 8 and 9. The best-predicted result was for Olive oil2, where all models achieved an accuracy exceeding 98%. In contrast, the lowest accuracy was observed for Olive oil3, which responded to all three models achieving less than 75% accuracy. Olive oil3 achieved the highest monounsaturated fatty acid content among the six brands of olive oil, which responded to 79%. However, the lowest monounsaturated fatty acid content was 70% referred to Olive oil4. The monounsaturated fatty acid content was a crucial indicator for evaluating the quality of olive oil. Meanwhile, it was also one of the primary components to distinguish olive oil from other edible oils, such as corn oil 28% and sunflower seed oil 23%. Therefore, it is suggested that OIRD method, combined with machine learning algorithms, can characterize the quality of olive oil.

 doi:10.20944/preprints202404.0285.v1

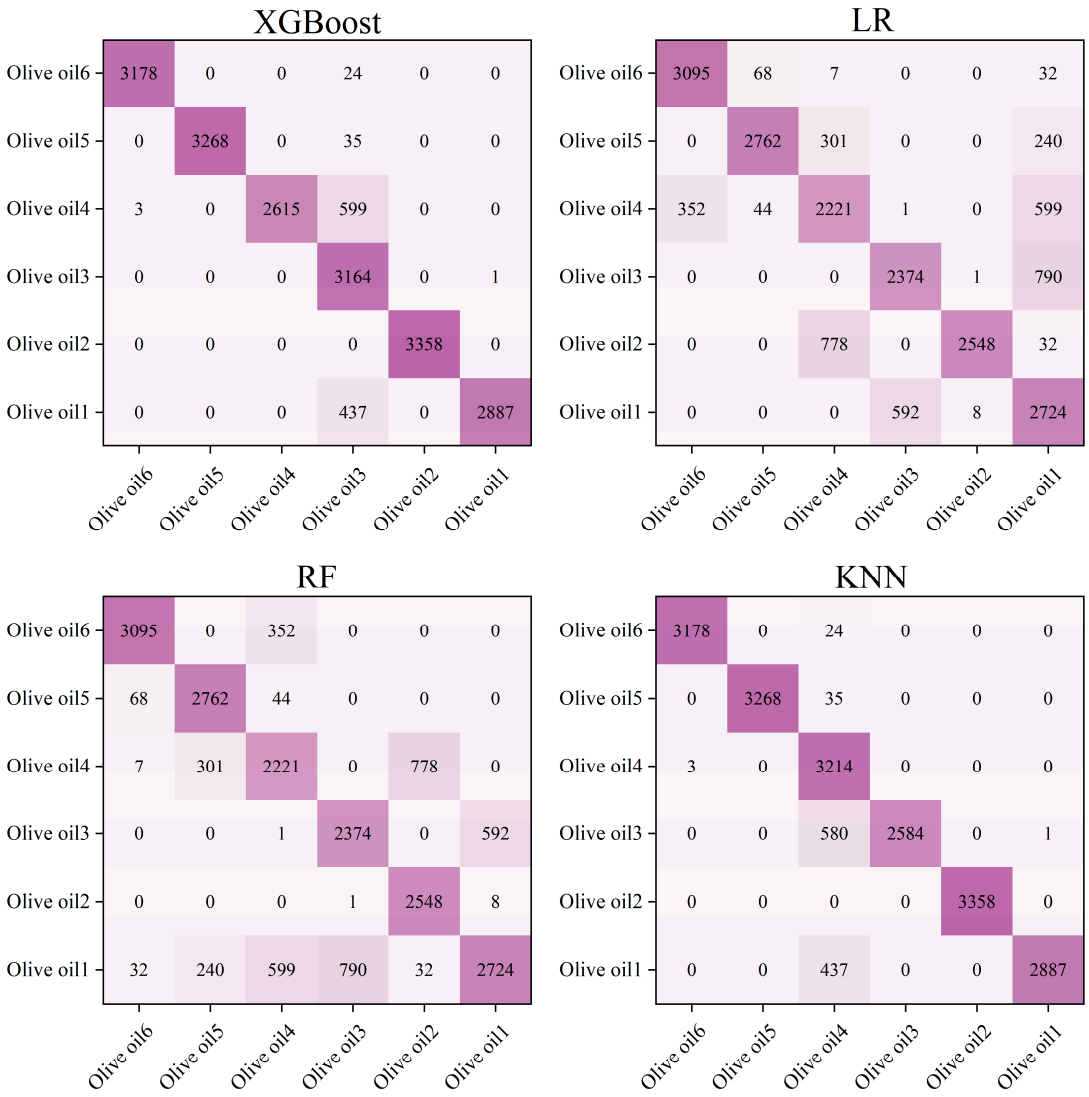

Figure 8. The confusion matrices for predicting the quality of olive oil using four models.

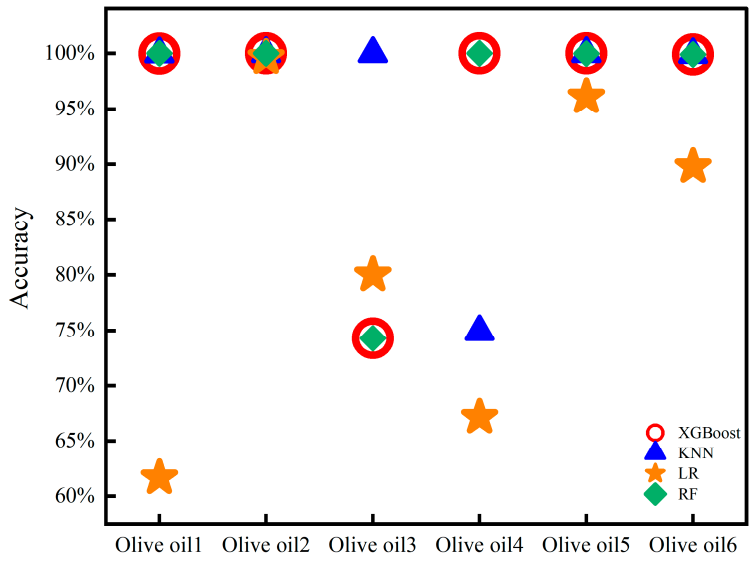

Figure 9. Accuracy of olive oil quality prediction.

 doi:10.20944/preprints202404.0285.v1

Except for Olive oil3, the prediction accuracy for olive oils exceeded 97%. The feature importance scores for the three signals were shown in the Figure 10. The contribution rates of OIRD, DC, and fundamental frequency signals to the classification results were 63.4%, 18.9%, and 17.6%, respectively. The feature importance score of the OIRD signal was significantly higher than that of the DC and fundamental frequency signals, indicating the feasibility of evaluating olive oil quality based on interface properties.

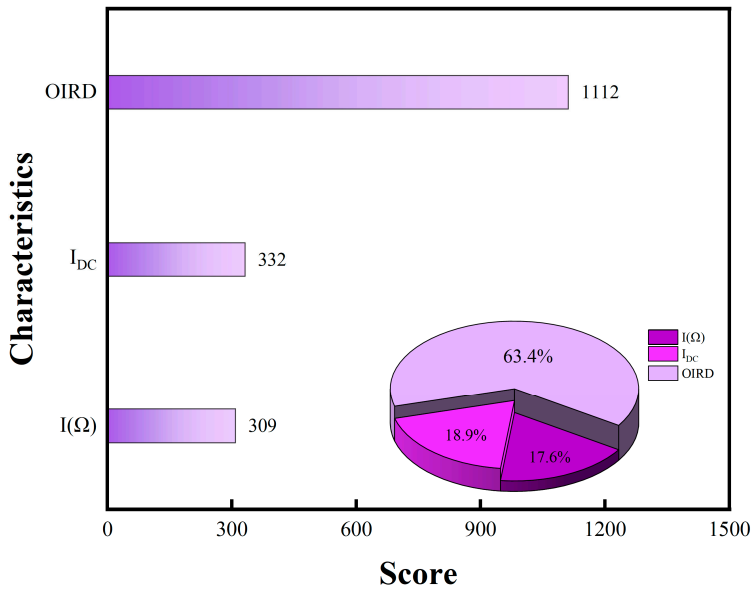

Figure 10. The feature importance scores for predicting the quality of olive oil using XGBoost.

Recently, the OIRD technique has been widely used in in monitoring in situ growth of oxide films[32–38], preparation of biochips[39–49], exploration of oil and gas resources[50–55]. Experimental results suggested that OIRD method can characterize the spatially resolved electrochemical reversibility of a polyaniline thin film. The OIRD signal would rise as the electrochemical conversion from completely reduced state to partially oxidized state[33]. Moreover, the deterioration of the electrochemical reversibility led to the decrease of OIRD signal. OIRD method was also been used in scanning of biomolecules, which can realize label-free detection of biological molecular interaction. Besides, based on the characterization of wax precipitation, the detection curve of OIRD can reveal the wax formation process.[50] In this paper, OIRD signals were used to guide models for the identification of edible oils. XGBoost, LR, RF and KNN algorithms were employed for quality analysis of the six olive oil samples. The Olive oil2 got the best-predicted result while the lowest accuracy was observed for Olive oil3. Besides, OIRD, DC and fundamental frequency signals exhibited different contribution rates to the classification results. Going forward, our work lays the groundwork for future efforts by researchers to use this work as the starting point for the application of OIRD in the characterization of edible oils.

4. Conclusions

In this work, OIRD method was used to characterize edible oils. DC signal, fundamental frequency signal, and OIRD signal were selected as features to establish prediction models, which based on XGBoost, LR, RF and KNN algorithms. The prediction accuracies of XGBoost, RF and KNN models all exceeded 95%. Moreover, compared to the fundamental frequency signal and DC signal, the contribution rate of the OIRD signal was significantly higher. Experimental results suggested that OIRD method can be a useful tool for the measurement of edible oils.

Author Contributions: Conceptualization, S.X.R. and H.Y.R.; methodology, S.X.R. and Z.K.; software, H.Y.R. and Y.S.N..; validation, S.X.R. and H.Y.R..; formal analysis, L.C.L.; investigation, Z.S.Z.; resources, L.X.C.; data

 doi:10.20944/preprints202404.0285.v1

curation, H.Y.R. and Y.S.N.; writing—original draft preparation, S.X.R. and H.Y.R..; writing—review and editing, Z.S.Z.; visualization, Z.K.; supervision, L.C.L.; project administration, S.X.R.; funding acquisition, S.X.R. and Z.K. All authors have read and agreed to the published version of the manuscript.

Funding: The corresponding author was supported by the National Natural Science Foundation of China under Grant 12374412 and the Beijing Natural Science Foundation under Grant 4222043.

Data Availability Statement: The original contributions presented in the study are included in the article/supplementary material, further inquiries can be directed to the corresponding author/s.

Acknowledgments: We thank Dr. Honglei Zhan, Dr. Xinyang Miao and Mr. Chao Song for their helpful discussion.

Conflicts of Interest: The authors declare no conflicts of interest.

References

1. Rajagukguk Y V, Cevoli C, Grigoletto I, et al. Rapid determination of the storage time of cold-pressed berry seed oils using flash gas chromatography E-Nose coupled with chemometrics. J FOOD ENG, 2024, 364: 111795
2. Roy M, Doddappa M, Yadav B K, et al. Detection of soybean oil adulteration in cow ghee (clarified milk fat): An ultrafast study using flash gas chromatography electronic nose coupled with multivariate chemometrics. J SCI FOOD AGR, 2022, 102(10): 4097-4108.
3. Kalo P, Kuuranne T. Analysis of free and esterified sterols in fats and oils by flash chromatography, gas chromatography and electrospray tandem mass spectrometry. J CHROMATOGR A, 2001, 935(1-2): 237-248.
4. Jing Q, Liu S, Song Y, et al. TaqMan real-time quantitative PCR for the detection of beef tallow to assess the authenticity of edible oils. FOOD CONTROL, 2024, 156: 110139.
5. Cui F, Liu M, Li X, et al. Gas chromatography ion mobility spectroscopy: A rapid and effective tool for monitoring oil oxidation. FOOD RES INT, 2024, 176: 113842
6. Geng D, Chen X, Lu D, et al. Discrimination of different edible vegetable oils based on GC-IMS and SIMCA. CYTA-J FOOD, 2023, 21(1): 49-56.
7. de Magalhães J B, Simon K F, Veiga E A, et al. Evaluating Adulteration of Commercial Extra Virgin Olive Oil with Canola and Sunflower Oils Through Electrochemical Impedance Spectroscopy. FOOD BIOPROCESS TECH, 2023: 1-13.
8. Jiménez A, Rufo M, Paniagua J M, et al. Temperature dependence of acoustic parameters in pure and blended edible oils: Implications for characterization and authentication. ULTRASONICS, 2024, 138: 107216.
9. Rolandelli G, Buera M P, Rodríguez S D. Monitoring thermal stability of pure and adulterated sesame oil using Fourier transform infrared spectroscopy and chemometric analysis. J FOOD COMPOS ANAL, 2024, 125: 105806.
10. Nagpal T, Yadav V, Khare S K, et al. Monitoring the lipid oxidation and fatty acid profile of oil using algorithm-assisted surface-enhanced Raman spectroscopy. FOOD CHEM, 2023: 136746.
11. Tang C, Qiao J, Wen Y, et al. Quality control of woody edible oil: The application of fluorescence spectroscopy and the influencing factors of fluorescence. FOOD CONTROL, 2022: 109275.
12. Gu H, Sun Y. A Rapid Method for Rapid Evaluation of Oil Quality Using Synchronous Fluorescence Spectroscopy. J NANOELECTRON OPTOE, 2018, 13(5): 743-748.
13. Poulli K I, Mousdis G A, Georgiou C A. Classification of edible and lampante virgin olive oil based on synchronous fluorescence and total luminescence spectroscopy. ANAL CHIM ACTA, 2005, 542(2): 151-156.
14. Songohoutou E E, Daniel L, Nouga A B, et al. Monitoringthe Thermal Oxidation of Local Edible Oils by Fluorescence Spectroscopy Technique Coupled to Chemometric Methods. FOOD ANAL METHOD, 2023, 16(8): 1422-1436.
15. Socaciu C, Fetea F, Ranga F, et al. Attenuated total reflectance-fourier transform infrared spectroscopy (ATR-FTIR) coupled with chemometrics, to control the botanical authenticity and quality of cold-pressed functional oils commercialized in Romania. FOOD ANAL METHOD, 2020, 10(23): 8695.
16. Su N, Pan F, Wang L, et al. Rapid detection of fatty acids in edible oils using vis-NIR reflectance spectroscopy with multivariate methods. BIOSENSORS-BASEL, 2021, 11(8): 261.
17. Mahboubifar M, Hemmateenejad B, Javidnia K, et al. Evaluation of long-heating kinetic process of edible oils using ATR–FTIR and chemometrics tools. J FOOD SCI TECH, 2017, 54: 659-668.
18. Zhuo-wei W, Jian-peng L, Xue-shi L, et al. Edible oil terahertz spectral feature extraction method combining radial basis function and KPCA. SPECTROSC SPECT ANAL, 2020, 40(2): 391-396.
19. Mei-tong N, De-gang X, Yu-ye W, et al. Investigation on characteristics of edible oil spectra with terahertz time-domain attenuated total reflection spectroscopy. SPECTROSC SPECT ANAL, 2018, 38: 2016-2020.

20. Cui-ling L, Yu-fei Y, Fang T, et al. Study on Quantitative Analysis of Edible Oil Peroxide Value by Terahertz Time Domain Spectroscopy. SPECTROSC SPECT ANAL, 2021, 41(5): 1387-1392.
21. Yin M, Tang S, Tong M. Identification of edible oils using terahertz spectroscopy combined with genetic algorithm and partial least squares discriminant analysis. ANAL METHODS-UK, 2016, 8(13): 2794-2798.
22. Ning H, Wang J, Jiang H, et al. Quantitative detection of zearalenone in wheat grains based on near-infrared spectroscopy. SPECTROCHIM ACTA A, 2022, 280: 121545.
23. Fakhri D, Khodayari A, Mahmoodzadeh A, et al. Prediction of Mixed-mode I and II effective fracture toughness of several types of concrete using the extreme gradient boosting method and metaheuristic optimization algorithms. ENG FRACT MECH, 2022, 276: 108916.
24. Xiong X, Guo X, Zeng P, et al. A short-term wind power forecast method via xgboost hyper-parameters optimization. FRONT ENERGY RES, 2022, 10: 905155.
25. Chen J, Zhao F, Sun Y, et al. Improved XGBoost model based on genetic algorithm. INT J COMPUT APPL T, 2020, 62(3): 240-245.
26. Dong A, Zhang Y, Guo Z, et al. Predicting the locations of missing persons in China by using NGO data and deep learning techniques. INT J DIGIT EARTH , 2024, 17(1): 2304076.
27. Ishwaran H, Malley J D. Synthetic learning machines. BIODATA MIN, 2014, 7: 1-12.
28. Wichitaksorn N, Kang Y, Zhang F. Random feature selection using random subspace logistic regression. EXPERT SYST APPL, 2023, 217: 119535.
29. Barker L, Brown C. Logistic regression when binary predictor variables are highly correlated. STAT MED, 2001, 20(9-10): 1431-1442.
30. Yang C Y, Ma Y W, Chen J L, et al. Novel Dynamic KNN with Adaptive Weighting Mechanism for Beacon-based Indoor Positioning System. J INTERNET TECHNOL, 2019, 20(5): 1601-1610.
31. Amat Sairin M, Abd Aziz S, Yoke Mun C, et al. Analysis and prediction of the major fatty acids in vegetable oils using dielectric spectroscopy at 5–30 MHz. PLOS ONE, 2022, 17(5): e0268827.
32. Zhu X. D., Lu H. B., Yang G. Z., et al. Epitaxial growth of SrTiO3 on SrTiO3(001) using an oblique-incidence reflectance-difference technique. PHYS REV B, 1998, 57:2514-2519.
33. Zhong C, Li L, Chen N, et al. Spatially resolved electrochemical reversibility of a conducting polymer thin film imaged by oblique-incidence reflectivity difference. CHEM COMMUN, 2020, 56(13): 1972-1975.
34. Chen F., Lu H. B., Zhao T., et al. Real-time optical monitoring of the heteroepitaxy of oxides by an oblique-incidence reflectance difference technique. PHYS REV B, 2000, 61(15):10404-10410.
35. Landry J. P., Zhu X. D., Gregg J. P.. Label-free detection of microarrays of biomolecules by oblique-incidence reflectivity difference microscopy. OPT LETT, 2004, 29(6):581-583.
36. Zhu X. D., James P. L., Sun Y. S., et al. Oblique-incidence reflectivity difference microscope for label-free high-throughput detection of biochemical reactions in a microarray format. APPL OPTICS, 2007, 46(10):1890-1895.
37. He L. P., Sun Y., Dai J., et al. Label-free and real-time detection of antigen-antibody interactions, by Oblique-incidence Reflectivity Difference (OIRD) method. SCI CHINA PHYS MECH, 2012, 55(9):1585-1588.
38. Lu H., Wen J., Wang X., et al. Detection of the specific binding on protein microarrays by oblique-incidence reflectivity difference method. J OPTICS-UK, 2010, 12(9):095301.
39. Zhang H, Xu M, Li H, et al. Detection speed optimization of the OI-RD microscope for ultra-high throughput screening. BIOMED OPT EXPRESS, 2023, 14(5): 2386-2399.
40. Zhu, C. G., Zhu, X. D., Landry, J. P., et al. Developing an efficient and general strategy for immobilization of small molecules onto microarrays using isocyanate chemistry. SENSORS-BASEL, 16(3), 378.
41. Zhu, C. G., Bilin G., Chen R., et al. Fast focal point correction in prism-coupled total internal reflection scanning imager using an electronically tunable lens. SENSORS-BASEL, 2018, 18(2):524.
42. Li Z. Y., Wang C., Wang Z. Y., et al. Allele-selective lowering of mutant HTT protein by HTT–LC3 linker compounds. NATURE, 2019, 575:203-209.
43. Wang J. Y., Dai J., He L. P., et al. Label-free and real-time detections of the interactions of swine IgG with goat anti-swine IgG by oblique-incidence reflectivity difference technique. J APPL PHYS, 2012, 112(6): 064702.
44. He L. P., Liu S., Dai J., et al. Label-free and real-time monitor of binding and dissociation processes between protein A and swine IgG by oblique-incidence reflectivity difference method. CHINESE PHYS LETT, 2015, 32(2): 020703.
45. Sun, Y. S. Use of Microarrays as a high-throughput platform for label-free biosensing. J LAB AUTOM, 2015, 20(4): 334-353.
46. Sun Y. S., Zhu X. D. Real-time, label-free detection of biomolecular interactions in sandwich assays by the oblique-incidence reflectivity difference technique. SENSORS-BASEL, 2014, 14(12): 23307-23320.
47. Hu S. H., Wan J., Su Y. J., et al. DNA methylation presents distinct binding sites for human transcription factors. ELIFE, 2013, 2(2):e 00726.
48. Li Z, Wang C, Wang Z, et al. Allele-selective lowering of mutant HTT protein by HTT–LC3 linker compounds. NATURE, 2019, 575(7781): 203-209.

 doi:10.20944/preprints202404.0285.v1

49. Liu H, Zhang H, Wu X, et al. Nuclear cGAS suppresses DNA repair and promotes tumorigenesis. NATURE, 2018, 563(7729): 131-136.
50. QING M, LIU J, HUANG Q, et al. In situ probing of wax precipitation of waxy oil using oblique-incidence reflectivity difference at open bulk surface. FUEL, 2022, 316: 123436.
51. Wang J., Zhan H. L., He L. P., et al. Evaluation of simulated reservoirs by using the oblique-incidence reflectivity difference technique. SCI CHINA PHYS MECH, 2016, 59(11):114221.
52. Zhan Honglei, Zhao Kun, Lu H. B., et al. Oblique-incidence reflectivity difference application for morphology detection. APPL OPTICS, 2017, 56(30): 8348-8352.
53. Zhan Honglei, Zhao Kun, Lu H. B., et al. In situ monitoring of water adsorption in active carbon using an oblique-incidence optical reflectance difference method. AIP ADV, 2017, 7:095219
54. Zhan H. L., Wang J., Zhao K., et al. Real-time detection of dielectric anisotropy or isotropy in unconventional oil-gas reservoir rocks supported by the oblique-incidence reflectivity difference technique. SCI REP-UK, 2016, 6(1): 39306.
55. Meng Z, Qin F, Li A, et al. Cluster structure of interfacial molecules studied by oblique incidence reflectance difference: Influences of salt ion on oil-water interfacial properties. J PETROL SCI ENG, 2023, 220: 111147.